DOI:
10.1016/j.mrgentox.2011.12.019

Document Version
Peer reviewed version

Merging nano-genotoxicology with eco-genotoxicology: An integrated approach to determine interactive genotoxic and sub-lethal toxic effects of C_{60} fullerenes and fluoranthene in marine mussels, *Mytilus sp*.

Sherain N. Al-Subiai[1]¶, Volker M. Arlt[2], Patricia E. Frickers[3], James W. Readman[3], Bjorn Stolpe[4], Jamie R. Lead[4], A. John Moody[1], Awadhesh N. Jha[1]*

[1]School of Biomedical & Biological Sciences, Plymouth University, Plymouth, PL4 8AA

[2]King's College London, School of Biomedical Science, Analytical and Environmental Science Division, Franklin-Wilkins Building, 150 Stamford Street, London SE1 9NH, UK

[3]Plymouth Marine Laboratory, Prospect Place, The Hoe, Plymouth PL1 3DH, UK

[4]School of Geography, Earth and Environmental Sciences, University of Birmingham, Birmingham, B15 2TT, U.K.

¶ Present address: Kuwait Institute of Scientific Research, Kuwait

* Correspondence: a.jha@plymouth.ac.uk

Telephone: +44-1752-584633; Fax: +44-1752-584605

Abstract

Whilst there is growing concern over the potential detrimental impact of engineered nanoparticles (ENPs) on the natural environment, little is known about their interactions with other contaminants. In the present study, marine mussels (*Mytilus sp.)* were exposed for 3 days to C_{60} fullerenes (C_{60}; 0.1-1 mg l^{-1}) and a model polycyclic aromatic hydrocarbon (PAH), fluoranthene (32-100 µg l^{-1}), either alone or in combination. The first two experiments were conducted by exposing the organisms to different concentrations of C_{60} and fluoranthene alone, in order to determine the effects on total glutathione level (as a measure of generic oxidative stress), genotoxicity (DNA strand breaks using Comet assay in haemocytes), DNA adduct analyses (using ^{32}P-postlabelling method) in different organs, histopathological changes in different tissues (i.e. adductor muscle, digestive gland and gills) and physiological effects (feeding or clearance rate). Subsequently, in the third experiment, a combined exposure of C_{60} plus fluoranthene (0.1 mg l^{-1} and 32 µg l^{-1}, respectively) was carried out to evaluate all endpoints mentioned above. Both fluoranthene and C_{60} on their own caused concentration-dependent increases in DNA strand breaks as determined by the Comet assay. Formation of DNA adducts however could not be detected for any exposure conditions. Combined exposure to C_{60} and fluoranthene additively enhanced the levels of DNA strand breaks along with a 2-fold increase in the total glutathione content. In addition, significant accumulation of C_{60} was observed in all organs, with highest levels in digestive gland (24.90 ± 4.91 µg C_{60} g^{-1} ww). Interestingly, clear signs of abnormalities in adductor muscle, digestive gland and gills were observed by histopathology. Clearance rates indicated significant differences compared to control with exposure to C_{60}, and C_{60} /fluoranthene combined treatments, but not after fluoranthene exposure alone. This study demonstrated that at the selected concentrations, both C_{60} and fluoranthene evoke toxic responses and genetic damage. The combined exposure produced enhanced damage with additive rather than synergistic effects.

Key words: Engineered nanoparticles (ENPs); C_{60} fullerenes***;*** Fluoranthene; DNA adducts, Comet assay, Histopathology; Clearance rate; Bivalve mollusc

1. Introduction

Manufactured or engineered nanoparticles (ENPs; size 1-100 nm) have in recent years captured the attention of scientific organisations, governments and industry worldwide. There has been much debate on the future environmental implications of ENPs as a result of their wide usage, as in paints, biocides, electronics, biomedicines, cosmetics and pharmaceuticals [1]. Given their widespread applications and intensified productions in the recent years, it is expected that aquatic environment and human(s) will be increasingly exposed to them. This warrants early evaluations of their potential environmental and health impacts [2, 3].

ENPs have different properties from their mother bulk analogues, due to the fact that they have a very large surface area to volume ratio. This feature could potentially result in (*a*) a high affinity for organic and metallic pollutants; (*b*) direct generation of reactive oxygen species (ROS); and (*c*) the ability to penetrate cells. A recent report by the European Agency for Safety and Health at Work [4] suggested that ENPs pose the strongest emerging risk to human health. EASW recommended that *in vivo* toxicological investigations are needed for nanomaterials to obtain more reliable data for risk assessment in order to meet European standard regulations. For the current study, Buckminster fullerenes or fullerenes (C_{60}) was chosen as it is an elementary component in many modern manufactured products. It is one of the most ubiquitous ENPs, generally present in polluted air as a result of fuel combustion [5].There have been concerns about the potential dermal and inhalation effects of C_{60}, due to its strong oxidizing and phototoxic properties [6]. In common with other ENPs, the potential health risk of C_{60} has however not been properly evaluated.

Fluoranthene is one of the most common pyrogenic polycyclic aromatic hydrocarbons (PAHs) and is present as a ubiquitous contaminant in human foods and in environmental samples [7]. The U.S. Environmental Protection Agency (EPA) has classified fluoranthene as one of the 16 priority PAHs. Its concentration in sediment has been found to range from tens to hundreds μg g^{-1} dry weight sediment [8]. Because fluoranthene can be metabolised by aquatic organisms it may generate reactive oxygen species (ROS) and form adducts, which can exert both acute toxic and genotoxic effects if antioxidant defences are overcome by pro-oxidant forces [9].

After ROS induction, a series of complex biological responses can be triggered by attack on DNA, proteins and lipid membranes [10]. The biological effects of C_{60} on its own however, appear to be contradictory. Whilst C_{60} has been shown to induce detrimental biological responses under *in vitro* and *in vivo* conditions, including on aquatic organisms using a range of parameters [11, 12, 13, 14, 15 16, 17, 18], other studies have suggested that it has no biological effects under different experimental conditions [19, 20]. Furthermore, investigations of the potential interaction of C_{60} with other contaminants have been very limited. Following two months of stirring in water, Baun et al. [21] suggested that 85% of phenanthrene, a model environmental toxicant, sorbed to C_{60}-aggregates and increased C_{60} toxicity in algae (*Pseudokirchneriella subcapitata*) and freshwater crustaceans, *Daphnia magna*. A preliminary study by Yang et al. [22] reported the effects of suspended C_{60} on the photo-induced toxicity of fluoranthene in *D. magna*. The study suggested that fluoranthene may be transported from the surface of the cage-like C_{60} structure to cross cell membranes. The authors further suggested that interactions between C_{60} and fluoranthene decrease both the uptake rate and increase the elimination rate for fluoranthene.

In the environment, organisms are generally exposed to mixtures of different contaminants or pollutants. These include combinations of organics, trace metals and ENPs [23, 24] which can interact in many ways (i.e. additively, synergistically, or antagonistically) to induce biological responses at different levels of biological organisation. However, investigations of the combined toxic effects of multiple chemicals on an animal are much more challenging than of a single compound [25], and are therefore sparse. For example, the number of possible combinations of pollutants is extremely large, and the combination that is likely to be most important is unkown. Moreover, it is more difficult to choose realistic ranges of exposure concentrations and the biological parameters to be tested than for a single pollutant.

In the current study, the role of C_{60} in contaminant delivery, and the potential effects of the interaction between C_{60} and fluoranthene on the living organism, was investigated using the filter feeder bivalve mussels, *Mytilus sp.* as a model organism. Mussels are known to exhibit measurable biochemical and behavioural end-points following exposure to toxicants. An integrated approach was adopted to

examine cellular and subcellular responses, as well as specific organ accumulation and the physiology to provide a more holistic assessment of the overall biological significance of such environmental variations. In addition to genotoxic effects in terms of DNA strand breaks (in haemocytes) and DNA adduct formation using ^{32}P-postlabelling method (in different tissues), the interactive effects were determined at several levels of the biological organisation. This included determination of total glutathione content (in adductor muscle), at the biochemical level; C_{60} accumulation and histopathology in adductor muscle, gills and digestive gland at the tissue and organ levels, and 'the clearance rate' as a measure of physiological effects at the organism level.

2. Materials & Methods

2.1. Chemicals

All chemicals and reagents were of high purity analytical grade and were obtained from Sigma-Aldrich (Poole, UK) unless stated otherwise.

2.2. Solution preparation

A primary stock solution (5.0 mg ml^{-1}) of fluoranthene was prepared in acetone. The fluoranthene concentration in the experimental exposure water was measured using solvent (dichloromethane) extraction with GC-Mass Spectrometry quantification (Agilent Technologies 6890 N Network GC system interfaced with an Agilent 5973 series mass selective detector). The C_{60} (lot number 11401DB; with purity 99.5% according to the manufacturer's information) was obtained from Sigma-Aldrich. The nanomaterial was dispersed in filtered (0.45 µm) seawater. The stock C_{60} suspensions (1 and 10 mg 10 ml^{-1}) were ultrasonicated (35 kHz frequency, Fisherbrand FB 11010) for 1 h to attempt uniform dispersion before adding to the exposure tanks to reach 0.1 and 1.0 mg l^{-1} C_{60}.

2.3. Characterisation of C_{60} nanoparticles

With limited characterisation data available for the commercial C_{60}, a broad analytical approach was applied to the concentrated stock suspension (10 mg l^{-1}). Hydrodynamic diameters, polydispersity index (PI) and zeta potential (surface

charges) of the C_{60} (100 mg l^{-1}) in filtered seawater were measured at 15°C using a Zetasizer Nano ZS ZEN3600 (Malvern Instruments Ltd., Malvern, UK) based on dynamic light scattering (DLS). The shapes and the sizes of the particles were also investigated using transmission electron microscopy (TEM, JEOL1200EX, 80 kV) and Atomic Force Microscopy (AFM, XE100, Park Systems) and the purity of the C_{60} was controlled by determining the element composition of discrete C_{60} particles using energy-dispersive X-ray diffraction and TEM (Philips Tecnai F20). Samples were prepared by drop deposition of C_{60} suspensions (10 mg l^{-1}) onto freshly cleaved muscovite (for AFM) and 300 mesh Cu-formvar grids (for TEM). The C_{60} particles were allowed to adsorb to muscovite for 5 min and to the TEM-grids for 30 min, after which the samples were washed by dipping into milli-Q water and air-dried overnight. Replicate samples were also prepared with fullerene dispersed in dichloromethane. Sample analyses were run in triplicate.

2.4. Animal collection and maintenance

Mussels (*Mytilus sp.*) of similar shell length (51-58 mm) were collected at low tide in April 2008 from Trebarwith Strand (Cornwall, UK), a relatively clean site (grid reference: SX048 866). These mussels were maintained under the standard laboratory conditions (mentioned below) until the end of June 2008 for 3 different sets of experiments. It should be pointed out that it had been assumed that mussels found around most of the coast of the UK, including in Cornwall, are *M. edulis*, whereas those found in the Mediterranean are *M. galloprovincialis*. Recently, however, using a molecular probe for the *Glu* gene, encoding an adhesion protein gene which demonstrates interspecies variation [26], it has been shown that the species composition of mussels at different sites in Devon and Cornwall (south west England) is quite variable and includes *M. edulis*, *M. galloprovincialis* and their hybrids [27]. At Trebarwith Strand, where our samples were collected, 97% of the organisms have been reported to be *M. galloprovincialis* and 3% to be hybrids [27]. Since the relative sensitivity of these two species to different contaminants has not been thoroughly investigated, and the species composition needs to be further confirmed using other markers with a larger sample size, it is appropriate to use the term *Mytilus sp.* in the present context, in line with other authors [28, 29, 30].

After collection, animals were immediately transported (in a cool box) to the laboratory where they were maintained in tanks under controlled conditions to acclimatize and used until the end of June 2008. During the experimental period, seawater quality was confirmed in each of the beakers by measuring % dissolved oxygen (96.1 ± 0.3%), pH (7.8 ± 0.02), total ammonia (0.04 ± 0.02 mg l^{-1}), temperature (15 ± 1°C) and salinity (31.5 ± 0.15 ‰) (Multi 340i/SET; WTW, Weilheim, Germany). A photoperiod of 12h light: 12h dark was maintained throughout.

2.5. Exposure conditions

The experiments were divided into 3 short-term (3 day) exposures to assess the toxicity of fluoranthene and C_{60}, both individually and in combination. This 3 day exposure period was based on earlier studies carried out in our laboratory which had shown genotoxic and physiological effects in this species following exposure to reference genotoxic agents [31, 32]. The first two experiments were conducted using differing levels of exposure to fluoranthene and C_{60} to evaluate potential dose response relationships for toxicological responses. Three animals from each beaker were taken and the tissues (i.e. adductor muscle, digestive gland and gills) were dissected and prepared for biochemical, histopathological and chemical analyses. Prior to dissection and collection of haemolymph samples, potential physiological effects were determined by 'clearance rate' assay. Animals were not fed during the experiment and all treatments were set up in triplicate.

2.5.1. Fluoranthene exposures

Initial experiments were designed to validate the sensitivity of the genotoxicity test (Comet assay) by using fluoranthene (3 day exposure) as a reference agent. The range of exposure concentrations for fluoranthene was chosen based on published results demonstrating lysosomal membrane damage in this species [33]. The concentration range used was, however, slightly modified to fit the semi-logarithmic scale widely applied in ecotoxicological studies [32, 34]. In 2 l glass beakers (3 animals $beaker^{-1}$), individuals were exposed to 32, 56, 100 µg l^{-1} fluoranthene. Exposure to solvent controls was also carried out; acetone (0.05 g ml^{-}

^{1}) was added instead of fluoranthene stock solution. The seawater was changed daily and re-dosed with appropriate quantities of the fluoranthene stock solutions.

2.5.2. C_{60} exposures

In 10 l glass tanks (10 animals per tank^{-1}) mussels were exposed to 0.1 and 1.0 mg l^{-1} C_{60} for 3 days. This concentration range was based on previous studies to evaluate lysosomal membrane stability as an indicator of cytotoxicity and other biological responses in adult and embryo-larval stages on bivalve and other aquatic species [12, 18]. In parallel to the exposure to C_{60}, exposure to 32 µg l^{-1} fluoranthene was also carried out as positive control. The seawater was changed daily and re-dosed with the appropriate concentration of C_{60}.

2.5.3. Combined exposures to C_{60} and fluoranthene

In a separate experiment (June 2008), mussels (n = 120) were divided into twelve 10 l glass tanks (10 animals tank^{-1}) with sea water. Three tanks were used per exposure group and mussels were exposed to 0.1 mg l^{-1} C_{60}, 32 µg l^{-1} fluoranthene and a mixture of C_{60} with fluoranthene at the same concentrations. The three remaining tanks were used as controls. In the experiment, two exposure durations were considered: three day exposure and three day post exposure in clean seawater, with removal of mussels at the end of each period for the analysis.

2.6. Collection of haemolymph samples and preparation of adductor muscle extract

From each individual mussel, approximately 0.20 ml of haemolymph was extracted from the posterior adductor muscle and was diluted with 0.20 ml physiological saline. Haemolymph-physiological saline suspension samples were centrifuged at 60 g_{av} in microfuge tubes for 2 min to pellet out the haemocytes which were then kept on ice for the Comet assay. Posterior adductor muscles from two mussels (approximately 0.2 g ww) were dissected and homogenized in extraction buffer (20 mM Tris-chloride, pH 7.6, containing 0.5 M sucrose and 1 mM EDTA) using a ratio of 1:3 (w/v) for total glutathione analysis as described by us in detail [35].

2.7. Determination of DNA strand breaks using the Comet assay

Haemocyte viability was checked using the Eosin Y assay. Single strand breaks in the mussels' haemocytes were determined using the alkaline Comet assay as described elsewhere [31, 32, 36]. The level of DNA damage in 100 cells sample^{-1} was measured by Komet 5.0 Image Analysis System (Kinetic Imaging, Liverpool, UK) using an epifluorescence microscope (Leica, DMR). Data for % tail DNA are presented as a reliable measure of single-strand DNA breaks/alkali labile sites [37].

2.8. DNA adduct analysis

DNA was isolated from digestive gland, gills and adductor muscle using a standard phenol/chloroform extraction method as described elsewhere [38]. DNA concentration and purity were determined spectrophotometrically using a NanoDrop^{TM}1000 spectrophotometer (USA). DNA adduct analysis for each DNA sample (4 µg) was carried out using the nuclease P1 enrichment version of the ^{32}P-postlabelling method as described previously [39, 40]. Resolution of ^{32}P-labelled adducts was carried out by chromatography on polyethyleneimine-cellulose (PEI-cellulose) thin-layer chromatography (TLC) sheets (10 × 20 cm, Macherey-Nagel, Düren, Germany) using the following solvents: D1, 1.0 M sodium phosphate, pH 6.0; D3, 4 M lithium-formate, 7 M urea, pH 3.5; D4, 0.8 M lithium chloride, 0.5 M Tris, 8.5 M urea, pH 8.0. TLC sheets were scanned using a Packard Instant Imager (Dowers Grove, IL, USA). An external anti-(±)-*trans*-7,8-dihydrooxy-9,10-epoxy-7,8,9,10-tetrahydrobenzo[*a*]pyrene (BPDE)-DNA standard [41] was employed as positive control.

2.9. Determination of total glutathione levels in adductor muscle extract

The total glutathione (i.e. reduced, GSH, and oxidised, GSSG) content of adductor muscle extract was determined essentially as described before [35]. The rate of absorbance decrease at 412 nm was measured using a microplate reader (Optimax, Molecular Devices, Sunnyvale, CA, USA) over 5 min using 96-well plates at 22℃.

2.10. Histological preparation for adductor muscle, digestive gland and gills

Tissues dissected from exposed animals (i.e. adductor muscle, digestive gland and gills) were examined by normal histological methods [36, 42, 43]. Each

organ was initially fixed in 10% buffered formal saline for at least 48 h. Specimens were then processed in ascending grades of alcohol. Tissue samples were embedded into paraffin and cut with a microtome at 5-7 µm thickness and mounted on slides. Slides were stained with haematoxylin and eosin (H and E) following Mayer's standard protocols.

2.11. Clearance rate

Clearance or feeding rates of individual mussel were determined as described elsewhere [32, 36, 43]. Briefly, mussels were allowed to acclimatise until their valves opened (approximately 10 min) prior to the addition of 500 µl of *Isochrysis* algal suspension (supplied by Cellpharm Ltd., Malvern, UK). The algae were mixed manually with a glass rod and then 20 ml of water sample was removed using a glass syringe. This procedure was repeated again after 20 min. Samples from both time zero and 20 min were analysed using a Beckham ^{TM} Coulter Particle Size and Count Analyser (Z2) to count particles between 4.0-10.0 µm in diameter. Clearance rate of the mussels were calculated based on the Coughlan (1969) equation as described elsewhere in detail [32, 36].

2.11. Chemical analyses of fluoranthene and C_{60}

2.11.1. GC-analysis of fluoranthene in water samples

Water samples were placed into glass vials with dichloromethane (DCM) in 1:9 ratio (v/v) and stored in darkness at –20 °C. Phenanthrene d_{10} (CAS: 1571-22-2) was added as an internal standard. Quantitative analyses of 1 µl aliquots of the DCM extracts were performed using an Agilent Technologies 6890 N Network GC system interfaced with an Agilent 5973 series mass selective detector. An HP-5MS (cross-linked 5% phenyl methyl siloxane) capillary column (30 m) with a film thickness of 0.25 µm and internal diameter 0.25 mm was used for separation, with helium as a carrier gas (maintained at a constant flow rate of 1 ml min^{-1}). Extracts were injected in splitless mode. Column temperature was programmed at 40 °C for 1 min, 40-300°C at 15°C per min and then held at 300°C for 5 min. Samples were screened for fluoranthene using selected ion monitoring (m/z 202) with quantification calculated relative to the phenanthrene d_{10} internal standard (monitored using m/z 188). Prior to

sample extract analyses, the system was calibrated using authentic standards. With each batch of samples, solvent and procedural blanks together with calibration standards were run in sequence.

2.11.2. HPLC-analysis of C_{60} in tissue samples

Adductor muscle, digestive gland and gills were carefully washed with pure toluene to remove surface adsorbed C_{60} particles. Then, tissues were extracted into toluene (1:9 w:v ratio) using ultra-sonication for 15 min (35 kHz frequency, Fisherbrand FB 11010). Extracts were centrifuged (9000 g_{av}) prior to HPLC analysis. C_{60} was separated using a Hypersil (5 µm) Elite C18 (250 × 4.6 mm I.D.) column. In the case of combined exposed samples (C_{60} and fluoranthene), a Plgel 5 µm 50 Å (manufactured by Agilent Technologies; USA) column was used to resolve the PAHs from the C_{60}. The mobile phase for both columns was toluene at a flow-rate of 1.0 ml min^{-1}. Sample injections were performed manually with volumes of 100 µl. The eluent was monitored at 330 nm using a Shimadzu SPD-6 AV UV–Vis spectrophotometer. Integration was performed using a Shimadzu-C-R3A chromatopac. For external calibration, a standard curve was generated for C_{60} concentrations ranging from 0.125 and 2.0 mg l^{-1}. The concentration of test sample was calculated by comparison to the standard curve.

2.12. Statistical analyses

Statistical analyses were performed using the statistical package StatGraphics plus, version 5.1 (Statistical Graphics Corp). All results are presented as mean ± S.E. Significant differences ($P < 0.05$) between groups were studied using one way analysis of variance (ANOVA) or Kruskal-Wallis test, followed by multiple range tests to differentiate between the groups of data.

3. Results

3.1. C_{60} characterisation

The DLS measurements of C_{60} in filtered seawater showed a large Z-average hydrodynamic diameter (680 ± 19 nm) and high polydispersity index (0.57),

indicating the formation of large agglomerates (Table 1). TEM micrographs of C_{60} particles in seawater and dichloromethane (Fig. 1a), and AFM images C_{60} in dichloromethane (Fig. 1b) showed aggregates that were composed of distinct particles. The purity of the C_{60} was assessed by TEM-EDX on 12 different C_{60} particles (example shown in Fig. 1c). No significant differences could be observed between EDX-spectra acquired on C_{60} particles and on the background carbon-coated Cu-grid (Fig. 1d), implying that element impurities were below the detection limit of EDX (typically 0.1 % of the total particle mass). The samples of C_{60} in dichloromethane were used for determination of particle sizes, since these gave TEM-micrographs with much higher contrast, and since the seawater samples gave AFM-images that were not consistent with the TEM-images, probably as a result of the extensive particle agglomeration in seawater. While the dichloromethane samples are not representative for the whole particle distribution in seawater (including agglomerates), they should give accurate sizes of discrete non-agglomerated particles. Size measurements of discrete particles within the agglomerates on the TEM micrographs and AFM images showed oval particles with diameters in the 100-200 nm range (Table 1). The difference in mean diameter given by TEM (160 nm) and AFM (122 nm) can be explained by the fact that the AFM height was measured as the height of particles above the muscovite surface, while the TEM diameter was measured along the surface of the grid.

3.2. Determination of DNA damage using the Comet assay

No significant loss of cell viability was observed for haemocytes (cell viability > 90% in all samples after Eosin Y staining) after exposure to fluoranthene, C_{60}, or C_{60} + fluoranthene (C_{60} + F) (data not shown). Since the Comet assay data were not normally distributed, the non-parametric Kruskal-Wallis test was applied to investigate significant differences between groups. Our results showed that there was a concentration-dependent response for fluoranthene (Fig. 2A). Also, in the second experiment significant differences were found between the control and C_{60} exposures (P = 0.0036) with higher DNA damage at 1.0 mg l^{-1} C_{60}-exposed animals (Fig. 2B). Multiple range tests (Fisher's LSD) showed a significant difference between all exposures. An equivalent DNA damage response was also observed

with the positive control (fluoranthene at 32 µg l^{-1}), indicating the robustness of the Comet assay.

3.2.2 DNA damage following combined exposures of C_{60} and fluoranthene

Mussels showed a significant elevation in DNA damage in exposed animals in comparison with the control for all the treatments alone or in combination (Fig. 2C). The results of the Comet assay for single and joint effects of C_{60} + F showed that combined exposure led to the highest DNA damage among the exposure experiments which was found to be additive rather than synergistic (Fig. 2C). After 3 day post-exposure, however, there was a significant decrease in DNA damage under all treatment conditions showing equal levels of damage in all the exposure conditions, but the decrease was greatest (approx. 3-fold) for the combined treatment of fluoranthene and C_{60}. Using 2-way ANOVA, a significant interaction was found between exposure type and time of measurement (P = 0.0001). Overall, these results indicate that the C_{60} interaction with PAHs contributes to the enhanced (i.e. additive) genotoxic effect in haemocytes and suggest that following both exposures (C_{60} and C_{60} + F), C_{60}-induced DNA damage recovered to the normal level after 3 day depuration.

3.3. Formation of DNA adducts

Under the chromatographic conditions used no DNA adducts were detectable in DNA samples obtained from adductor muscle, digestive gland and gills either from single exposure to C_{60} and fluoranthene or the combined exposure (Fig. 3).

3.4. Determination of total glutathione levels in adductor muscle

As shown in Figure 4A, C_{60} exposure resulted in a slight increase in the total glutathione content (i.e. reduced, GSH and oxidised, GSSG, combined) in adductor muscle in comparison to the control, but the effect was not significant. On the other hand, a significant increase (P < 0.05, ANOVA) in total glutathione levels was reported in C_{60} + F-exposed animals. An approximately 2-fold increase in total glutathione content was seen in the adductor muscle after exposure to the C_{60} and fluoranthene mixture in comparison to other groups. Multiple range tests (Fisher's LSD) showed significant differences at the 95% confidence level, between the C_{60} +

F and fluoranthene exposure alone (Fig. 4B). Total glutathione levels in control samples from the C_{60} + F experiment were lower than the control from the C_{60} experiment, but this effect could be attributed to laboratory acclimatisation of the mussels at higher temperature (i.e. 15º C) as the two experiments were carried out at different times (i.e. 6 weeks part) after their collection from the field.

3.5. Histopathological observations

Table 2 summarises the main histopathological abnormalities in different treatment groups. Histological examinations indicated that there were no pathological alterations in control specimens. However, different tissues showed varying degrees of abnormalities (e.g. haemocyte infiltration, necrosis or other injuries) following exposures (Fig. 5). Adductor muscle samples from the 'C_{60} exposure' group did not show any histological abnormalities at 0.1 mg l^{-1} C_{60}, but at 1.0 mg l^{-1} C_{60} caused atrophy in myocyte cells and a decrease in extracellular spaces between muscle bundles in three (i.e. 33%) out of nine examined animals (Fig. 5B). Similar effects were also observed with the adductor muscle exposed to combined exposure of C_{60} + fluoranthene, with even more adverse effects; six (i.e. 66%) animals showed abnormalities including two (i.e. 22%) animals showing hypertrophy (swelling) and loss of muscle bundle organisation (Fig. 5C; Table 2), and another four (i.e. 44%) animals had muscle atrophy and decreased extracellular spaces between muscle bundles.

The histological observations in the digestive gland specimens showed that C_{60} exposure caused alterations in the digestive tubules (Fig. 5E; Table 2). Low C_{60} exposure (0.1 mg l^{-1}) caused loss of definition of the digestive tubules, probably caused by necrosis in three (i.e. 33%) out of nine specimens, whereas the other six (i.e. 66%) specimens exhibited clear signs of necrosis in the digestive tubules. These effects were even more pronounced when fluoranthene interacted with C_{60} in the combined exposure. Histological changes were characterised by necrosis in digestive cells within the digestive tubules and were observed in all animals examined. We found atrophy of the digestive tubule epithelium in which the epithelium cells shrank and exhibited thin tubules, only basement membrane remained and cellular debris was often observed within the lumen of the digestive tubules (Fig. 5F; Table 2).

Histological examination of the gills revealed that 0.1 mg l^{-1} C_{60} caused abnormalities. Two (i.e. 22%) mussels at the low C_{60} concentration showed signs of hypoplasia in frontal and lateral cilia. Progressively more abnormalities were seen with high C_{60} exposure (1.0 mg l^{-1}); 4 (i.e. 44%) animals out of 9 had hypoplastic effects in the frontal and lateral cilia (Fig. 5H). Gills examined after C_{60} + F exposure showed areas with erosion of cilia and filament necrosis in 3 (i.e. 33%) out of 9 specimens (Fig. 5I; Table 2).

3.6. C_{60} accumulation

In order to understand the pattern of C_{60} accumulation in mussel tissues, after 3 day exposure, adductor muscle, digestive gland and gills were analyzed for C_{60} content using HPLC. Results are shown in Figure 6A. The ranking of organs according to increasing C_{60} concentrations was identical at both exposure concentrations: adductor muscle < gills < digestive gland. No significant difference was found between C_{60} levels in the adductor muscle in comparison to the control. Gills displayed a significant accumulation of C_{60} in animals exposed to 0.1 mg l^{-1} C_{60}, but no significant difference was observed with the higher exposure (P = 0.15, ANOVA). In contrast, significant differences in C_{60} levels were found with 0.1 and 1.0 mg l^{-1} exposures for digestive gland (ANOVA; P = 0.04 and P = 0.03, respectively), with the highest C_{60} concentrations measured in the 1.0 mg l^{-1} exposed animals (24.90 ± 4.91 µg C_{60} g^{-1} ww). Thus, the digestive gland appears to be the most important target tissue/repository for C_{60}.

Results of the C_{60} accumulation in the combined exposure experiment are summarised in Fig. 6 B, C and D. It appears that C_{60} accumulated more in animals exposed to C_{60} alone than those exposed to C_{60} + F. Whilst a significant increase in C_{60} accumulation is shown following exposure, after 3 day depuration there was a significant decrease in C_{60} content both in the digestive gland and gills.

3.7. Clearance rate (CR)

The CR data measured in mussels exposed to C_{60} (Fig. 7A) showed that mussels exposed to 1.0 mg l^{-1} C_{60} were significantly affected (P < 0.05, ANOVA). Whilst not significant, a reduction in CR is also indicated for animals exposed to 0.1

mg l^{-1} (P = 0.0002, t-test). Mussels exposed to the combination of C_{60} with fluoranthene also showed a significant decrease in CR (P = 0.017, t-test; Fig. 7B). It should be noted, however, that the clearance rates in control animals from the 'C_{60} + F' experiment was lower than in the 'C_{60}' experiment, possibly indicating a slight decline in health with time, although the clearance rate for C_{60} exposure alone in both sets of exposures were comparable. After 3 days depuration, CRs of both C_{60} and C_{60} + fluoranthene increased significantly, indicating that the feeding activity of the mussels had, to an extent, recovered.

4. Discussion

In common with other environmental contaminants, interactive effects of C_{60} and ubiquitous organic contaminants, such as fluoranthene, represent an area of research that has not yet been fully covered. As mentioned earlier, despite having strong oxidizing and phototoxic properties [6], the potential detrimental effects of C_{60} on its own and in combination with other agents are inadequately studied and are therefore inconclusive in the literature [44]. Using mammalian systems, either no cytotoxic, mutagenic effects [20, 45, 46] or positive responses for the induction of DNA and cellular damage [11, 47, 48], have been reported. In this context, it is generally accepted that the toxic potential of ENPs is not only dependent upon its quality, but also on target cell types, quality, purity and synthesis method of the ENPs, and treatment of the cells [49, 50, 51, 52]. While determining the induction of DNA damage and other toxicological parameters, it is also very important that the methodologies have been thoroughly optimised and validated against reference genotoxic and toxic agents to ensure the assay is reliable, reproducible and sensitive [34, 53, 54]. In this context, the endpoints analysed in this study were thoroughly optimised and validated in this model system before evaluating the toxic potential of C_{60} and fluoranthene either alone or in combination [36]. Where appropriate, concurrent positive controls were also used in the experimental design to make the results robust.

Prior to evaluation of the potential detrimental biological responses of ENPs, their physico-chemical properties were thoroughly quantified as recommended [50,

51]. The zeta potential of C_{60} in filtered seawater was a relatively small negative charge, indicating that the fullerenes are unlikely to be fully stabilised. This colloidal instability was confirmed by DLS, TEM and AFM where large agglomerates were recorded. However, the DLS data for polydisperse agglomerate samples are only qualitative [55], since the DLS sensitivity increases rapidly with particle size, and must therefore be treated with caution. However, taken together, the characterisation data show that the C_{60} were composed of 100-200 nm particles (indicated by AFM and TEM) that were present both as a discrete particles and formed agglomerates of several hundred nm in seawater (indicated by DLS). These results are expected from un-functionalised commercial fullerenes.

Previous *in vivo* studies have evaluated C_{60}-induced oxidative stress in the embryonic stage of zebrafish, suggesting that it can act as a pro-oxidant and enhance toxic response by interacting with biomolecules such as DNA, proteins and lipids [17]. This is broadly in line with positive responses observed in our study for the Comet assay following exposure to C_{60} on its own, but is in contrast to the study of Jacobson et al., [46], who could not find a positive response in the same assay in mouse lung epithelial cells. Whilst there is some information on potential effects of C_{60} in mammalian systems, data is limited for aquatic organisms. For interactive effects, a preliminary study reported that the toxicity of phenanthrene on the fresh water flea (*D. magna*) increased significantly in the presence of C_{60} [21]. It was assumed that phenanthrene is only bioavailable form [21], but that C_{60} aggregates acted to deliver the phenantherene to the cell membrane, where it is known to have a targeted narcotic effect [21]. If this hypothesis is accepted, the apparent induction of DNA damage in our study could be a result of oxidative stress, resulting in lipid peroxidation of the cell membrane, as lipid peroxidation has been positively linked with induction of DNA damage [56]. Relative contributions of C_{60} and fluoranthene for the generation of free radicals however could be difficult to speculate as mentioned below, PAHs are also known to generate ROS. Similarly, Yang et al. [22] also reported the effects of suspended C_{60} on the photo-induced toxicity of fluoranthene in *D. magna*. The study suggested that fluoranthene may be transported from the surface of the cage-like C_{60} structure to cross the cell membranes. Once inside the cells, varieties of mechanisms could lead to generation of different qualities and quantities of free radicals leading to induction of genetic damage [57, 58]. In addition,

other indirect mechanisms of genotoxicity (i.e. via interaction of the contaminants with non-DNA targets) could also result in observed genotoxic effects.

Besides the reported toxic effect of ENPs, either directly or through generation of ROS [1], many studies have shown that PAHs such as fluoranthene in addition to binding with the biomolecules (i.e. forming adducts) have the ability to produce ROS resulting in induction of oxidative damage [9, 33, 59, 60, 61]. In the absence of formation of any bulky DNA adducts in different tissues, our results indicate that C_{60} and fluoranthene cause DNA damage, possibly by generating ROS. This could however only be confirmed using a modified Comet assay to quantify oxidised purines and pyrimidines, as carried out by us using fish cells under in vitro and in vivo conditions [49, 62, 63]. In this context, however, it has also been suggested that antibacterial activity of fullerene water suspensions is not due to ROS-mediated damage [15]. Due to technical and logistic limitations (mainly the amount of haemolymph samples required for modified Comet assay depending upon the number of bacterial enzymes and animals to be used, increased number of samples and sampling times), determination of oxidative DNA damage could not be carried out in our study. As a measure of global oxidative stress however, as mentioned earlier and discussed later, levels of total glutathione from the adductor muscle extracts were determined. This assay has been thoroughly optimised and validated in our laboratory conditions [35, 36]. The observed recovery of induced DNA damage in the post-exposure period in the combined exposure experiments (i.e. C_{60} + fluoranthene) could be explained by either an enhanced repair process when the mussels were returned to the clean seawater or as a result of enhanced turnover rate of haemocytes. Similar observations have been made in other studies following exposure to environmental contaminants [64].

At the biochemical level, combined exposure of C_{60} plus fluoranthene caused a significant increase in glutathione levels in the adductor muscle which further indicates an induction of oxidative stress, and reflects the increased DNA damage in the haemocytes and histological changes in different tissues. Even where there was evidence of uptake of C_{60} into adductor muscle (Fig. 6B), this was not associated with elevated glutathione levels except in the combined exposure with fluoranthene indicating that C_{60} alone did not cause oxidative stress in this tissue. In a previous

study, we found that adductor muscle is a useful tissue to determine biomarker responses to oxidative stress. Elevated levels of glutathione in adductor muscle of *Mytilus edulis* have been reported by us after 5 day acute exposure to Cu (40 µg l^{-1}) [35]. A possible explanation for this induction is that under exposure conditions mussels tend to activate γ-glutatmyl-cysteine synthetase (GCS) to restore glutathione levels (GSH synthesis is regulated in part by a non-allosteric competitive feedback inhibition of GCS by GSH). If this activation is maintained for several days, GSH levels could increase as suggested by Yan et al. [65]. Peña-Llopis and co-workers [66] found that a higher muscular GSH or GSH/GSSG ratio can be expected in mussels after long fenitrothion exposure. Different results on glutathione content have been obtained for organisms exposed to different types of chemical compounds. In common with other biological responses, the variability in these investigations may be due to a number of intrinsic and extrinsic factors including the C_{60} treatment regime (exposure time and nanomaterial preparation), the cell type or organisms used, as well as the metabolic/antioxidant capacity of the organism [43]. As estimation of glutathione levels in mussels in our laboratory conditions has been optimised and validated extensively [35, 36], we attribute the significant differences observed for enhanced levels of glutathione in combined exposures (i.e. F+C_{60}) to acclimatisation of mussels at higher temperature (i.e. 15ºC) in the laboratory conditions following their collection from the natural environment. Both impact of temperature and seasons on enzyme activities in mussels and other aquatic organisms is well documented, accounting for disparity in observed biomarker responses following exposure to contaminants [67-69]. This acclimatisation of mussels in our study had however no detrimental effects on the overall physiology of the mussels as in both sets of experiments (i.e. C_{60} and combined exposures), C_{60} alone treatment had comparable levels of clearance rate.

Highly reactive metabolites following exposure to PAHs can lead to covalent binding with DNA forming DNA adducts. The presence of DNA adducts following dietary exposure (50 mg kg^{-1} dw) to benzo[*a*]pyrene have previously been reported in mussels [70]. Another study also showed tissue specific differences in DNA adduct formation in *M. galloprovincialis* collected from PAH-contaminated sites [71]. However, in the present investigation, *in vivo* exposure to 32 µg l^{-1} fluoranthene for 3 day did not reveal any DNA adduct formation in any of the tested organs. In mussels,

there is a general lack of information on the potential formation of DNA adducts either by fluoranthene or C_{60}. The possible explanation of our results is that either fluoranthene was not able to form DNA adducts in mussel or that the experimental conditions used for ^{32}P-postlabelling were not sensitive enough to detect them. It however should be pointed out that DNA-adduct analysis using ^{32}P-postlabelling method was used to detect bulky adducts and not oxidised bases, which would result from oxidative stress. Absence of any bulky DNA adduct further supports the notion that under the experimental conditions oxidative stress is mainly responsible for observed biological responses.

After the biochemical and cellular changes, a sequence of biological responses at higher order of biological organisation which included histopathological and physiological alterations was observed in the exposed mussels. In addition, C_{60} accumulation in different tissues was also observed. The effects of C_{60} were investigated in the tissues that are indicative of the overall health of the organism (adductor muscle), metabolism (liver) or absorption (gills). Adductor muscle exhibited a clear adverse atrophy in myocyte cells in C_{60} plus fluoranthene exposed animals which led to weak muscle bundle structure and therefore decreased extra-cellular spaces of connective tissue. De Oliveira Ribeiro et al., [72] also found similar effects in the muscles of adult male zebrafish following exposure to methyl mercury. They found a decrease of the space between fibre bundles and disorganisation of myofibrils. No studies have however reported potential histopathological changes of the adductor muscle in mussels after exposure to ENPs. Further, gills and digestive gland tissues showed marked degenerative changes. In gills of C_{60} plus fluoranthene-exposed mussels, ciliary erosion and necrosis of filaments were observed. Similar toxic effects were noticed previously in mussels exposed to other toxicants including heavy metals [36, 73]. As mussel gills are critical organs for their respiratory and osmoregulatory functions, injuries in gill tissues may reduce the oxygen consumption and impair the physiological function of the organ. The apparent reductions in clearance rate observed in the current study are probably the result of ciliary erosion which leads to the failure in physiological processes in the whole organism [74]. Moreover, C_{60} exposure caused reduction in digestive tubule thickness (tubule atrophy) as a result of loss of digestive and basophilic secretory cells within the lumen of digestive tubules. The effects of C_{60} were enhanced when

fluoranthene was added, with even more severe changes observed in digestive tubules. The digestive gland of the exposed mussels showed necrosis (diffuse nuclei and no clear distinction in some epithelial cells), adverse atrophy of digestive tubule and stomach epithelium. Weinstein [75] found that oysters (*Crassostrea virginica)* exposed to 100 µg l^{-1} fluoranthene in the laboratory for 21 days also exhibit a reduction in their mean digestive epithelial thickness. Digestive gland tissue of mussel is an important organ for active metabolism and detoxification and is extremely sensitive to pollutants [76]. Histological changes in the digestive tubules have been used to assess the effects of environmental contaminants [27,77, 78] and in common with other observations, it could be suggested that C_{60}-and fluoranthene-induced histopathological changes are not unique and quantitatively or qualitatively they often do not show concentration-dependent changes as observed in earlier studies [36,43]. Despite the fact that under laboratory conditions it has not been possible to induce neoplasia in invertebrates including bivalve molluscs [43, 54], neoplasia has been reported in bivalve molluscs from different parts of the world often correlated with exposures to environmental contaminants [43, 79]. The gross histopathological changes observed in our study could however be indicative of factors that promote neoplastic development in these organisms [80].

Chemical analyses of mussels exposed to C_{60} alone showed predominant accumulation of C_{60} in the digestive gland with more modest accumulation in the gill. In contrast, lower accumulation of C_{60} was found in tissues from animals co-exposed to C_{60}/fluoranthene. Accumulation of C_{60} was influenced by co-exposure to fluoranthene; animals exposed to C_{60} alone accumulated more C_{60} than combined exposed mussels. It is also interesting to note that whilst the uptake was higher in C_{60} only exposures, the biological responses indicate that combined exposures were more effective in inducing detrimental effects. In line with limited information pertaining to potential interactive toxic effects of ENPs with other contaminants [21, 22], it appears that C_{60} could act as *Trojan Horses* in facilitating the uptake of fluoranthene and enhancing the biological responses or conversely fluoranthene can enhance the toxicity of C_{60}. It is also worth mentioning that limited data are available in the literature showing differential patterns of tissue-specific accumulation, according to single or co-contaminant exposures. For example, whilst co-exposure of phenanthrene in C_{60} suspensions showed higher bioaccumulation of phenanthrene

(no C_{60} was measured) [21], another study using mussels showed that gold nanoparticles (GNPs) are better accumulated when used alone, whereas no GNPs were detectable in tissues when used in combination with menadione, a pro-oxidant [81]. Despite being metallic ENPs, in line with our observations, the GNPs predominantly accumulated in digestive glands and modestly in gills with no accumulation in mantle. Interestingly, no trace of gold was found in tissues from animals co-exposed to GNPs/ menadione [81]. The authors conclude that, as a consequence of the menadione toxicity, accumulation of GNPs may be impaired during feeding. Some minor peaks in the chromatograms of our study were also observed in the digestive gland and gill tissue samples, indicating that some metabolites could be produced over the exposure period. Understanding of toxicokinetics and metabolites for C_{60} and fluoranthene would greatly help to explain the tissue/ organ- specific damage. There has however been very limited study in aquatic invertebrates as a whole to elucidate toxicokinetics for organic contaminant uptake and tissue-specific deposition to link with tissue specific damage [43]. From an ecotoxicological perspective, while the study has been carried out using adult life stages of the mussels, it is also important to evaluate the sensitivity of early life stages of this species [82] and establish relative sensitivity with other ecologically important species [54, 83, 84].

5. Conclusions

Our experimental results confirm that exposures of mussels to both fluoranthene and C_{60} on their own result in concentration-dependant increases in DNA strand breaks but there was no evidence of DNA adduct formation under the experimental conditions. We show, for the first time, that combined exposures enhance the levels of DNA strand breaks and elevate total glutathione levels indicating oxidative stress to the exposed organisms. The effects at lower levels of biological organisation also become more pronounced at higher levels in terms of histopathological and physiological changes. Following this study involving short term exposures, longer exposure times are now required to further explore the potential effects of ENPS, either alone or in combination with other contaminants. Our integrated study adds to very limited information available on the potential impact of ENPs on aquatic biota and underlines the advantages of using filter-

feeding organisms in future investigations of environmental effects of manufactured or engineered nanomaterials at the whole organism level. This approach could be translated to other ecologically relevant species to assess the ecotoxicological impact of ENPs.

Acknowledgements

SNAI-S has been supported by Kuwait Institute for Scientific Research (KISR), State of Kuwait. VMA is supported by Cancer Research UK. ANJ acknowledges support from European Regional Development Fund, INTERREG IVA (grant n. 4059). We would also like to acknowledge funding from the Natural Environment Research Council (NERC), UK via the Facility for Environmental Nanoscience Analysis and Characterisation (FENAC).

References:

[1] N. Singh, B. Manshian, G.J.S. Jenkins, S.M. Griffiths, P.M. Williams, T.G.G. Maffeis, C.J. Wright, S.H. Doak, NanoGenotoxicology: The DNA damaging potential of engineered nanomaterials, Biomaterials. 30 (2009) 3891-3914.
[2] M.N. Moore, Do nanoparticles present ecotoxicological risks for the health of the aquatic environment? Environ. Int. 32, (2006) 967-976.
[3] T.M. Scown, R. van Aerle, C.R. Tyler, Review: Do engineered nanoparticles pose a significant threat to the aquatic environment?, Critical Reviews in Toxicology. 40 (2010) 653-670.
[4] EASW. Approaches to safe nanotechnology, Managing the health and safety concerns associated with engineered nanomaterials. (2009).
[5] G.D. Nielsen, M. Roursgaard, K.A. Jensen, S.S. Poulsen, S.T. Larsen, In vivo Biology and toxicology of fullerenes and their derivatives, Basic. Clin. Pharmacol. 103 (2008) 197-208.
[6] C.S. Foote, F.N. Diederich, R. Whetten, F. Wudl, Buckminsterfullerene. (1990) Chm. Eng. News 2.
[7] D.H. Phillips, Polycyclic aromatic hydrocarbons in the diet, Mutat. Res. 443 (1999) 139-147.
[8] J.P. Gao, J. Maguhn, P. Spitzauer, A. Kettrup, Distribution of polycyclic aromatic hydrocarbons (PAHs) in pore water and sediment of a small aquatic ecosystem, Int. J. Environ. An. Ch. 69 (1998) 227-242.
[9] A. Palmqvist, L.J. Rasmussen, V.E. Forbes, Influence of biotransformation on trophic transfer of the PAH, fluoranthene, Aquat. Toxicol. 80 (2006) 309-319.
[10] D.M. Guldi, M. Prato, Excited-state properties of C_{60} fullerene derivatives, Accounts. Chem. Res. 33 (2000) 695-703.
[11] A. Dhawan, J.S. Taurozzi, A.K. Pandey, W. Shan, S.M. Miller, S.A. Hashsham, V.V. Tarabara, stable colloidal dispersions of C_{60} fullerenes in water: evidence for genotoxicity, Environ. Sci. Technol. 40 (2006) 7394-7401.

[12] A.H. Ringwood, N. Levi-Polyachenko, D.L. Carroll, Fullerene exposures with oysters: embryonic, adult, and cellular responses, Environ. Sci. Technol. 43 (2009) 7136-7141.
[13] E. Oberdörster, Manufactured nanomaterials (fullerenes, C_{60}) induce oxidative stress in brain of juvenile largemouth bass., Environ. Health. Pers. 112 (2004) 1058-1062.
[14] G. Oberdörster, E. Oberdörster, J. Oberdörster, nanotoxicology: an emerging discipline evolving from studies of ultrafine particles., Environm. Health Persp. 113 (2005) 823-839.
[15] D.Y. Lyon, L. Brunet, G.W. Hinkal, M.R. Wiesner, P.J.J. Alvarez, Antibacterial activity of fullerene water suspensions (nC_{60}) is not due to ROS-mediated damage, Nano Lett. 8 (2008) 1539-1543.
[16] S. Zhu, E. Oberdörster, M.L. Haasch, Toxicity of an engineered nanoparticle (fullerene, C_{60}) in two aquatic species, Daphnia and fathead minnow, Mar. Environ. Res. 62 (2006) S5-S9.
[17] C.Y. Usenko, S.L. Harper, R.L. Tanguay, Fullerene C60 exposure elicits an oxidative stress response in embryonic zebrafish, Toxicol. Appl. Pharmacol. 229 (2008) 44-55.
[18] M.N. Moore, J.A.J. Readman, J.W. Readman, D.M. Lowe, P.E. Frickers, A. Beesley, Lysosomal cytotoxicity of carbon nanoparticles in cells of the molluscan immune system: An in vitro study, Nanotoxicology. 3 (2009) 40-45.
[19] P. Spohn, C. Hirsch, F. Hasler, A. Bruinink, H.F. Krug, P. Wick, C60 fullerene: A powerful antioxidant or a damaging agent? The importance of an in-depth material characterization prior to toxicity assays, Environ. Pollut. 157 (2009) 1134-1139.
[20] N. Shinohara, K. Matsumoto, S. Endoh, J. Maru, J. Nakanishi, In vitro and in vivo genotoxicity tests on fullerene C_{60} nanoparticles, Toxicol Lett. 191 (2009) 289-296.
[21] A. Baun, S.N. Sørensen, R.F. Rasmussen, N.B. Hartmann, C.B. Koch, Toxicity and bioaccumulation of xenobiotic organic compounds in the presence of aqueous suspensions of aggregates of nano-C_{60}, Aquat. Toxicol. 86 (2008) 379-387.
[22] X.Y. Yang, R.E. Edelmann, J.T. Oris, Suspended C60 nanoparticles protect against short-term UV and fluoranthene photo-induced toxicity, but cause long-term cellular damage in *Daphnia magna*, Aquat. Toxicol. 100 (2010) 202-210.
[23] A.B.A. Boxall, K. Tiede, Q. Chaudhry, Engineered nanomaterials in soils and water: how do they behave and could they pose a risk to human health?, Nanomedicine. 2 (2007) 919-927.
[24] K.R. Echols, J.C. Meadows, C.E. Orazio, E.L. Gene, Pollution of aquatic ecosystems II: hydrocarbons, synthetic organics, Radionuclides, heavy metals, acids, and thermal pollution. Encyclopedia of Inland Waters. Oxford: Academic Press. p 120-128, (2009).
[25] M. Benedetti, G. Martuccio, D. Fattorini, A. Canapa, M. Barucca, M. Nigro, F. Regoli, Oxidative and modulatory effects of trace metals on metabolism of polycyclic aromatic hydrocarbons in the Antarctic fish *Trematomus bernacchii*. Aquat. Toxicol. 85 (2007)167-175.
[26] K. Inoue, W.J. Herbert, M. Matsuoka, S. Odo, S. Harayama, Interspecific variations in adhesive protein sequence of Mytilus edulis, M. galloproviancialis and M. trossulus. Biol. Bull. 189 (1995) 370-375.
[27] J.P. Bignell, G.D. Stentiford, N.G.H. Taylor, B.P. Lyons, Histopathology of mussels (*Mytilus sp.*) from the Tamar estuary, UK, Mar. Environ. Res. 72 (2011) 25-32.

[28] M. Banni, A. Negri, M. Rebelo, F. Rapallo, H. Boussetta, A. Viarengo, F. Dondero, Expression analysis of the molluscan p53 protein family mRNA in mussels (*Mytilus spp.*) exposed to organic contaminants, Comp. Biochem. C. 149 (2009) 414-418.
[29] E. Kádár, D. Lowe, M. Solé, A. Fisher, A. Jha, J. Readman, T. Hutchinson, Uptake and biological responses to nano-Fe versus soluble $FeCl_3$ in excised mussel gills, Anal. Bioanal. Chem. 396 (2010) 657-666.

[30] J.P. Shaw, F. Dondero, M.N. Moore, A. Negri, A. Dagnino, J.W. Readman, D.R. Lowe, P.E. Frickers, A. Beesley, J.E. Thain, A. Viarengo, Integration of biochemical, histochemical and toxicogenomic indices for the assessment of health status of mussels from the Tamar Estuary, U.K, Mar. Environ. Res. 72 (2011) 13-24.
[31] A.N. Jha, Y. Dogra, A. Turner, G.E. Millward, Impact of low doses of tritium on the marine mussel, *Mytilus edulis*: Genotoxic effects and tissue-specific bioconcentration, Mutat. Res. 586 (2005) 47-57.
[32] M.N. Canty, T.H. Hutchinson, R.J. Brown, M.B. Jones, A.N. Jha, Linking genotoxic responses with cytotoxic and behavioural or physiological consequences: Differential sensitivity of echinoderms (*Asterias rubens*) and marine molluscs (*Mytilus edulis*), Aquat.Toxicol. 94 (2009) 68-76.
[33] D.M. Lowe, C. Soverchia, M.N. Moore, Lysosomal membrane responses in the blood and digestive cells of mussels experimentally exposed to fluoranthene, Aquat. Toxicol. 33 (1995) 105-112.
[34] A.N. Jha, T.H. Hutchinson, J.M. Mackay, B.M. Elliot, D.R. Dixon, Development of an in vivo genotoxicity assay using the marine worm *Platynereis dumerilii* (Polychaeta: Nereidae), Mutat. Res. 359 (1996) 141-150.
[35] S.N. Al-Subiai, A.N. Jha, A.J. Moody, Contaminantion of bivalve haemolymph samples by adductor muscle components: implications for biomarkers studies, Ecotoxicology 18 (2009) 334-342.
[36] S.N. Al-Subiai, A.J. Moody, S.A. Mustafa, A.N. Jha, A multiple biomarker approach to investigate the effects of copper on the marine bivalve mollusc, *Mytilus edulis*, Ecotoxicol. Environ. Safe. 74 (2011) 1913-1920.
[37] T.S. Kumaravel, A.N. Jha, Reliable Comet assay measurements for detecting DNA damage induced by ionising radiation and chemicals, Mutat. Res. 605 (2006) 7-16.
[38] B.C. Jaeschke, G.E. Millward, A.J. Moody, A.N. Jha, Tissue-specific incorporation and genotoxicity of different forms of tritium in the marine mussel, *Mytilus edulis*, Environ. Pollut. 159 (2011) 274-280.
[39] V.M. Arlt, M. Stiborová, C.J. Henderson, M. Thiemann, E. Frei, D. Aimová, R. Singh, G. Gamboa da Costa, O.J. Schmitz, P.B. Farmer, C.R. Wolf, D.H. Phillips, Metabolic activation of benzo[a]pyrene in vitro by hepatic cytochrome P450 contrasts with detoxification in vivo: experiments with hepatic cytochrome P450 reductase null mice, Carcinogenesis. 29 (2008) 656-665.
[40] D.H. Phillips, V.M. Arlt, The 32P-postlabeling assay for DNA adducts, Nat. Protocols. 2 (2007) 2772-2781.
[41] D.H. Phillips, M. Castegnaro, o.b.o.t.t. participants, Standardization and validation of DNA adduct postlabelling methods: report of interlaboratory trials and production of recommended protocols, Mutagenesis. 14 (1999) 301-315.
[42] S. Sheir, R. Handy, Tissue injury and cellular immune responses to cadmium chloride exposure in the common mussel *Mytilus edulis* modulation by lipopolysaccharide, Arch. Environ. Con. Tox. 59 (2010) 602-613.

[43] Y. Di, D.C. Schroeder, A. Highfield, J.W. Readman, A.N. Jha, Tissue-specific expression of *p53* and *ras* genes in response to the environmental genotoxicant benzo(α)pyrene in marine mussels. Environ. Sci. Technol. 45 (2011) 8974-8981.
[44] R. Landsiedel, M.D. Kapp, M. Schulz, K. Wiench, F. Oesch, Genotoxicity investigations on nanomaterials: Methods, preparation and characterization of test material, potential artifacts and limitations-Many questions, some answers, Mutat. Res. 681 (2009) 241-258.
[45] J. Mrđanović, S. Šolajić, V. Bogdanović, K. Stankov, G. Bogdanović, A. Djordjevic, Effects of fullerenol C_{60}(OH)24 on the frequency of micronuclei and chromosome aberrations in CHO-K1 cells, Mutat. Res. 680 (2009) 25-30.
[46] N.R. Jacobsen, G. Pojana, P. White, P. Møller, C.A. Cohn, K. Smith Korsholm, U. Vogel, A. Marcomini, S. Loft, H. Wallin, Genotoxicity, cytotoxicity, and reactive oxygen species induced by single-walled carbon nanotubes and C60 fullerenes in the FE1-Muta™Mouse lung epithelial cells, Environ. Mol. Mutagen. 49 (2008) 476-487.
[47] A. Xu, Y. Chai, T. Nohmi, T.K. Hei, Genotoxic responses to titanium dioxide nanoparticles and fullerene in gpt delta transgenic MEF cells, Part Fibre Toxicol. 6 (2009) 3.
[48] J.K. Folkmann, L. Risom, N.R. Jacobsen, H. Wallin, S. Loft, P. Moller, Oxidatively damaged DNA in rats exposed by oral gavage to C60 fullerenes and single-walled carbon nanotubes, Environmen Health Perspect. 117 (2009) 703-708.
[49] W.F. Vevers, A.N. Jha, Genotoxic and cytotoxic potential of titanium dioxide nanoparticles on fish cells in vitro. Ecotoxicology. 17 (2008) 410-420.
[50] R. Handy, F. von der Kammer, J. Lead, M. Hassellöv, R. Owen, M. Crane, The ecotoxicology and chemistry of manufactured nanoparticles, Ecotoxicology. 17 (2008) 287-314.
[51] Y. Ju-Nam, J.R. Lead, Manufactured nanoparticles: An overview of their chemistry, interactions and potential environmental implications, Sci.Total Environ. 400 (2008) 396-414.
[52] S.H. Doak, S.M. Griffiths, B. Manshian, N. Singh, P.M. Williams, A.P. Brown, G.J.S. Jenkins, Confounding experimental considerations in nanogenotoxicology, Mutagenesis. 24 (2009) 285-293.
[53] F. Atienzar, A. Evenden, A. Jha, D. Savva, M. Depledge, Optimized RAPD analysis generates high-quality genomic DNA profiles at high annealing temperature, Biotechniques. 28 (2000) 52-54.
[54] A.N. Jha, Ecotoxicological applications and significance of the comet assay, Mutagenesis. 23 (2008) 207-221.
[55] R.F. Domingos, M.A. Baalousha, Y. Ju-Nam, M.M. Reid, N. Tufenkji, J.R. Lead, G.G. Leppard, K.J. Wilkinson, Characterizing manufactured nanoparticles in the environment: multimethod determination of particle sizes, Environ. Sci. Technol. 43 (2009) 7277-7284.
[56] L.J. Marnett, Lipid peroxidation-DNA damage by malonialdehyde. Mutat. Res. 424, (1990) 83-95.
[57] N.J.F. Dodd, A.N. Jha, Titanium dioxide induced cell damage: A proposed role of the carboxyl radical, Mutat. Res. 660 (2009) 79-82.
[58] N.J.F. Dodd, A.N. Jha, Photoexcitationof aqueous suspensions of titanium dioxide nanoparticles: an electron spin resonance spin trapping study of potentially oxidative reactions, Photochem. Photobiol. 87 (2011) 632-640.

[59] J.A. Coles, S.R. Farley, R.K. Pipe, Effects of fluoranthene on the immunocompetence of the common marine mussel, *Mytilus edulis*, Aquat. Toxicol. 30 (1994) 367-379.
[60] G.R. Lotufo, Bioaccumulation of sediment-associated fluoranthene in benthic copepods: uptake, elimination and biotransformation. Aquat. Toxicol. 44 (1998) 1-15.
[61] E.L. Cavalieri, E.G. Rogan, Central role of radical cations in metabolic activation of polycyclic aromatic hydrocarbons, Xenobiotica. 25 (1995) 677-688.
[62] J.F. Reeves, S.J. Davies, N.J.F. Dodd, A.N. Jha, Hydroxyl radicals (OH) are associated with titanium dioxide (TiO_2) nanoparticle-induced cytotoxicity and oxidative DNA damage in fish cells, Mutat. Res. 640 (2008) 113-122.
[63] S.A. Mustafa, S.N. Al-Subiai, S.J. Davies, A.N. Jha, Hypoxia-induced oxidative DNA damage links with higher level biological effects including specific growth rate in common carp, *Cyprinus carpio* L, Ecotoxicology. 20 (2011) 1455–1466.
[64] D. Tran, A.J. Moody, A.S. Fisher, M.E.Foulkes, A.N.Jha, Protective effects of selenium on mercury-induced DNA damage in mussel haemocytes. Aquatic Toxicol. 84 (2007) 11-18.

[65] T. Yan, L.H. Teo, Y.M. Sin, Effects of mercury and lead on tissue glutathione of the green mussel, *Perna viridis*, Bull. Environ. Contam.Toxicol. 58 (1997) 845-85.

[66] S. Peña-Llopis, M.D. Ferrando, J.B. Peña, Impaired glutathione redox status is associated with decreased survival in two organophosphate-poisoned marine bivalves, Chemosphere. 47 (2002) 485-497.
[67] N. Bodin, T. Burgeot, J.Y. Stanisiere, G. Bocquene, D. Menard, C. Minier, I. Boutet, A. Amat, Y. Cherel, H. Budzinski, Seasonal variations of a battery of biomarkers and physiological indices for the mussel *Mytilus galloproviancialis* transplanted into the northwest Mediterranean Sea, Comp. Biochem. Physiol. Part C. 138 (2004) 411-427.

[68] V.I.Lushchak, T.V. Bagnyukova, Temperature increase results in oxidative stress in goldfish tissues. 1. Indices of oxidative stress, Comp. Biochem & Physiol. Part C 143 (2006) 30-35.

[69] V.I.Lushchak, T.V. Bagnyukova, Temperature increase results in oxidative stress in goldfish tissues. 2. antioxidant and associated enzymes, Comp. Biochem & Physiol. Part C 143 (2006) 36-41.
[70] F. Akcha, C.I. zuel, P. Venier, H. Budzinski, T. Burgeot, J.F. Narbonne, Enzymatic biomarker measurement and study of DNA adduct formation in benzo[a]pyrene-contaminated mussels, *Mytilus galloprovincialis*, Aquat. Toxicol. 49 (2000) 269-287.
[71] M. Pisoni, L. Cogotzi, A. Frigeri, I. Corsi, S. Bonacci, A. Iacocca, L. Lancini, F. Mastrototaro, S. Focardi, M. Svelto, DNA adducts, benzo(a)pyrene monooxygenase activity, and lysosomal membrane stability in *Mytilus galloprovincialis* from different areas in Taranto coastal waters (Italy), Environ.Res. 96 (2004) 163-175.
[72] C.A. de Oliveira Ribeiro, M.-D. Nathalie, P. Gonzalez, D. Yannick, B. Jean-Paul, A. Boudou, J.C. Massabuau, Effects of dietary methylmercury on zebrafish skeletal muscle fibres, Environ.Toxicol. Pharmacol. 25 (2008) 304-309.
[73] I. Sunila, Acute histological responses of the gill of the mussel, *Mytilus edulis*, to exposure by environmental pollutants. J. Inverteb. Pathol. 52 (1988) 137-141.

[74] M.A. Gregory, D.J. Marshall, R.C. George, A. Anandraj, T.P. McClurg, Correlations between metal uptake in the soft tissue of *Perna perna* and gill filament pathology after exposure to mercury, Mar. Pollu. Bull. 45 (2002) 114-125.
[75] J.E. Weinstein, Fluoranthene-induced histological alterations in oysters, Crassostrea virginica: Seasonal field and laboratory studies, Mar. Environ. Res. 43 (1997) 201-218.
[76] D.R. Livingstone, Cytochrome P-450 in pollution monitoring use of cytochrome P-450 1A (CYP1A) as a biomarker of organic pollution in aquatic and other organisms. Richardson M, editor. London, UK: Taylor & Francis. 143–160 p, 1996.
[77] M. Auffret, Histopathological changes related to chemical contamination in *Mytilus edulis* from field and experimental conditions, Mar. Ecol-Prog Ser. 46 (1988) 101-107.
[78] D.M. Lowe, R.K. Pipe, Mortality and quantitative aspects of storage cell utilization in mussels, *Mytilus edulis*, following exposure to diesel oil hydrocarbons, Mar. Environ. Res. 22 (1987) 243-251.
[79] C.M. Ciocan, J.M. Rotchell, Conservation of cancer genes in the marine invertebrate *Mytilus edulis*, Environ. Sci.Techn. 39 (2005) 3029-3033.
[80] J. Vakkila, M.T. Lotze, Inflammation and necrosis promote tumour growth, Nat. Rev. Immunol. 4 (2004) 641-648.
[81] S. Tedesco, H. Doyle, J. Blasco, G. Redmond, D. Sheehan, Exposure of the blue mussel, *Mytilus edulis*, to gold nanoparticles and the pro-oxidant menadione, Comp. Biochem. C. 151 (2010) 167-174.
[82] J.A. Hagger, F.A. Atienzar, A.N. Jha, Genotoxic, cytotoxic, developmental and survival effects of tritiated water in the early life stages of the marine mollusc, *Mytilus edulis*, Aquat. Toxicol. 74 (2005) 205-217.
[83] A.N. Jha, J.A. Hagger, S.J. Hill, M.H. Depledge, Genotoxic, cytotoxic and developmental effects of tributyltin oxide (TBTO): an integrated approach to the evaluation of the relative sensitivities of two marine species, Mar. Environ. Res. 50 (2000) 565-573.
[84] V.V. Cheung, M.H. Depledge, A.N. Jha, An evaluation of the relative sensitivity of two marine bivalve mollusc species using the Comet assay, Mar. Environ. Res. 62 (2006) S301-S305.

Figure legends & Table captions

Fig. 1 Characterisation of C_{60} fullerenes particles; (A) TEM micrograph, (B) AFM image, (C) EDX-spectrum of C_{60}-particle, (D) EDX-spectrum from the background.

Fig. 2 Induction of DNA strand breaks, represented as %Tail DNA in mussel haemocytes following 3 days *in vivo* exposure to: (A) fluoranthene (32, 56 and 100 µg l^{-1}); (B) C_{60} (0.1 and 1.0 mg l^{-1}); and (C) C_{60} + fluoranthene (0.1 mg l^{-1} C_{60} and 32 µg l^{-1} fluoranthene). The values are mean ± S.E. Bars with the same letters are not significantly different whereas different letters show significant difference from other treatment ($P < 0.05$) according to the multiple range test (LSD). +ve control= 32 µg l^{-1} fluoranthene; F = fluoranthene; C60 = C_{60} fullerenes; F+C60 = fluoranthene+ C_{60} fullerenes.

Fig. 3 ^{32}P-post labelling analysis of DNA from cells exposed to C_{60} fullerenes (C_{60}), fluoranthene and C_{60} + fluoranthene. DNA adduct profiles measured in digestive gland. Same results were obtained with gills and adductor muscle. BPDE = anti-(±)-*trans*-7, 8-dihydrooxy-9,10-epoxy-7,8,9,10-tetrahydrobenzo[*a*]pyrene.

Fig. 4 Total glutathione levels in the adductor muscle extract following 3 days *in vivo* exposure to: (A) C_{60}; and (B) mixture of C_{60} + fluoranthene (0.1 mg l^{-1} C_{60} and 32 µg l^{-1} fluoranthene). The values are mean ± S.E. Bars with the same letters are not significantly different whereas different letters show significant difference from other treatment ($P < 0.05$) according to the multiple range test (LSD). F = fluoranthene; C60 = C_{60} fullerenes; F+C60 = fluoranthene+ C_{60} fullerenes.

Fig. 5 Haematoxylin and eosin (H & E) light micrographs of 5-8 µm thick sections through adductor muscle, digestive gland and gills of *M. edulis* showing the histological structure of control and treated mussels. A, D & G: control; B, E & H: exposed to C_{60}: C, F & I: exposed to C_{60} + fluoranthene. mc = myocyte cell; si = sinus; dc = digestive cell; pbc = pyramidal basophilic secretory cell; dd = digestive diverticula; gf = gill filaments; fc = frontal cilia; lc = lateral cilia; ge = gill epithelium; dt = digestive tubules; at = atrophy; n = necrosis; hypo = hypoplasia; e = erosion. Scale bar: 100 µm.

Fig. 6 C_{60} concentrations in tissues. (A) accumulation of C_{60} in adductor muscle, digestive gland and gills after exposure to 0.1 & 1.0 mg l-1. (B, C & D) accumulation of C_{60} after exposure to mixture of C_{60} + fluoranthene (adductor muscle, digestive gland and gills, respectively). Data are mean ± S.E., n = 3 mussel per treatment after 3 days of exposure. Bars with the same letters are not significantly different whereas different letters show significant difference from other treatment ($P < 0.05$) according to the multiple range test (LSD). F = fluoranthene; C60 = C_{60} fullerenes; F+C60 = fluoranthene+ C_{60} fullerenes.

Fig. 7 Clearance rate (represent as l h^{-1}) in *Mytilus* sp. following 3 days *in vivo* exposure to: (A) C_{60} (0.1 & 1.0 mg l^{-1}), and (B) mixture of C_{60} + fluoranthene (0.1 mg l^{-1} C_{60} and 32 µg l^{-1} fluoranthene). The values are mean ± S.E. Bars with the same letters are not significantly different whereas different letters show significant difference from other treatment ($P < 0.05$) according to the multiple range test (LSD). F = fluoranthene; C60 = C_{60} fullerenes; F+C60 = fluoranthene+ C_{60} fullerenes.

Table captions

Table 1

Results showing characterisation measurements of C_{60} fullerenes particles using different techniques. Values are mean ± S.E.

Table 2

Summary of histopathological evaluations of different organs of mussels, *Mytilus* sp. following exposure to C_{60} fullerenes (C_{60}) and fluoranthene, either alone or in combination.

Fig. 1 Characterisation of C_{60} fullerenes particles; (A) TEM micrograph and (B) AFM image

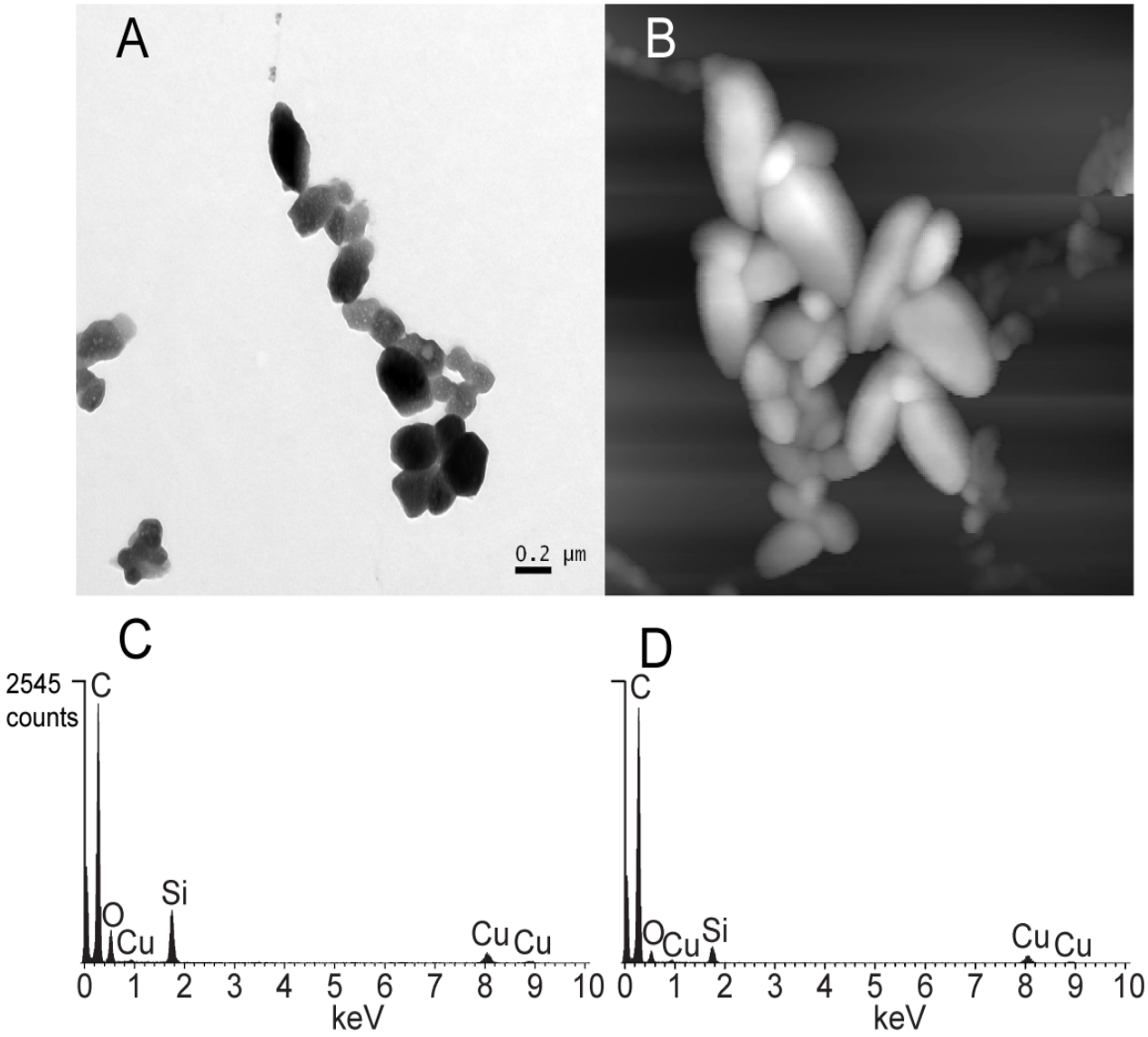

Fig. 2

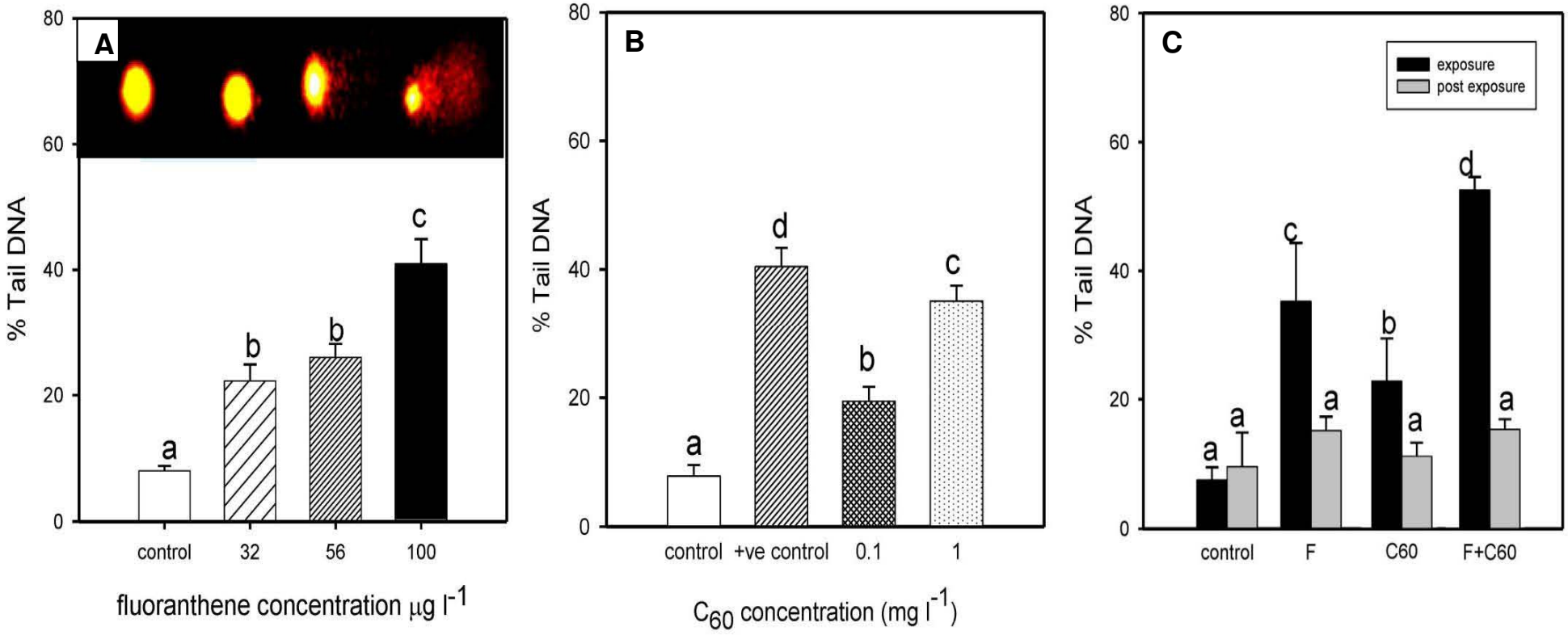
A
% Tail DNA
80
60
40
20
0
a
b
b
c
control
32
56
100
fluoranthene concentration µg l-1
B
% Tail DNA
a
d
b
c
control
+ve control
0.1
1
C60 concentration (mg l-1)
C
exposure
post exposure
a
a
c
a
b
a
d
a
control
F
C60
F+C60

Fig 3.

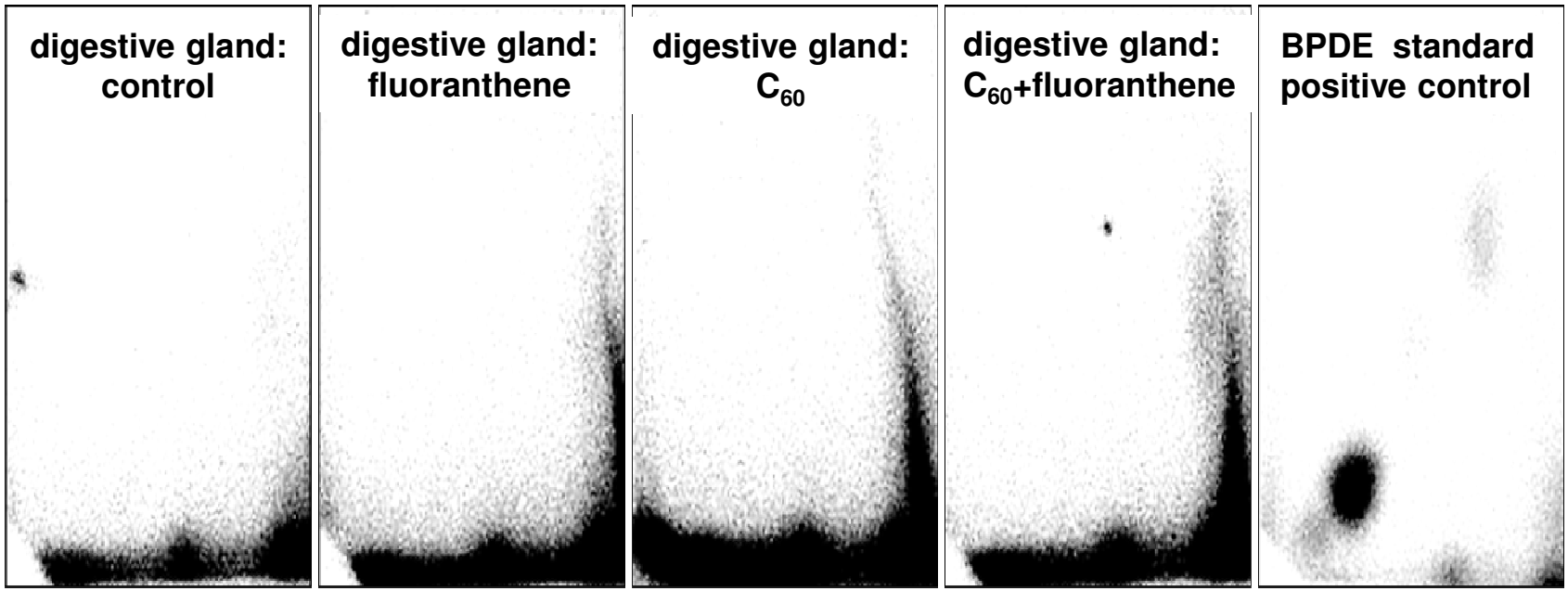
digestive gland: control
digestive gland: fluoranthene
digestive gland: C_{60}
digestive gland: C_{60}+fluoranthene
BPDE standard positive control

Fig. 4

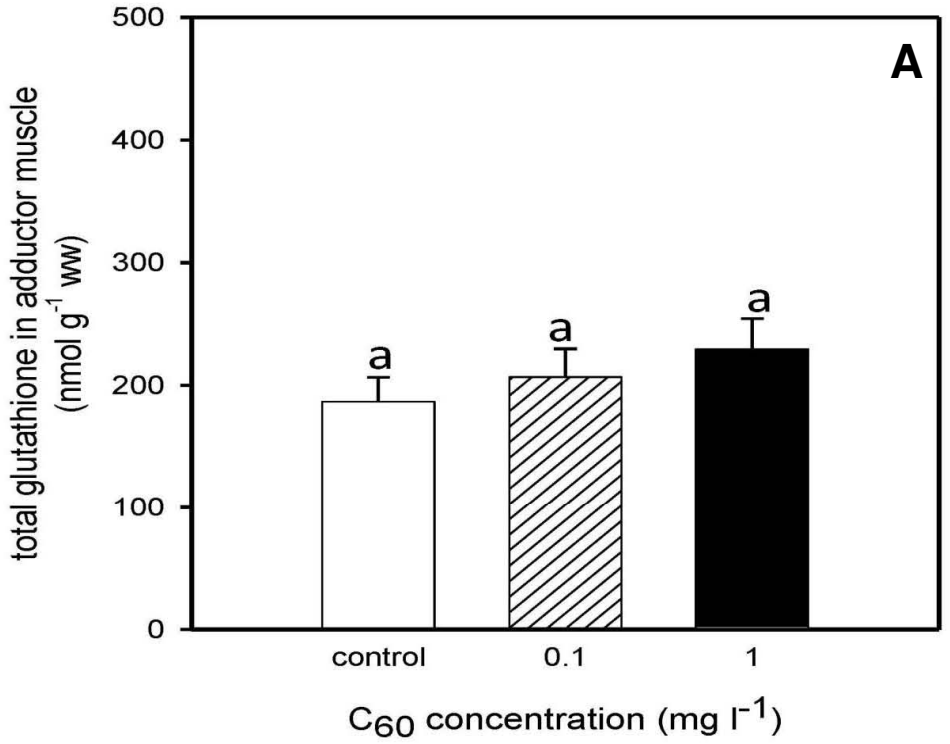
A
total glutathione in adductor muscle (nmol g-1 ww)
500
400
300
200
100
0
a
a
a
control
0.1
1
C60 concentration (mg l-1)

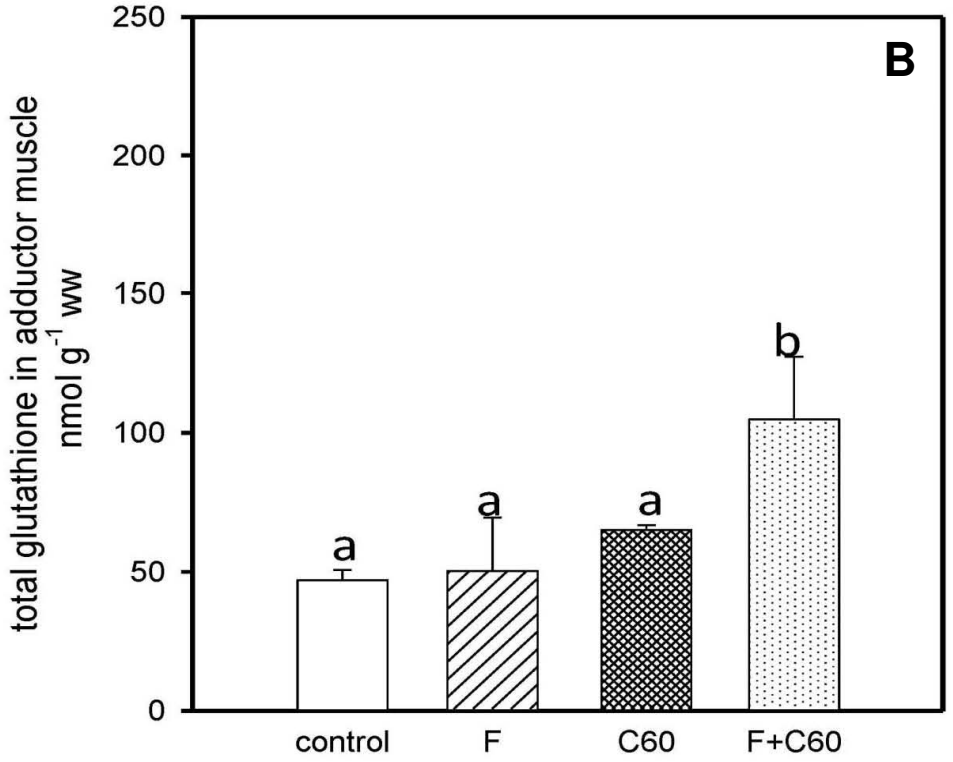
B
total glutathione in adductor muscle nmol g-1 ww
250
200
150
100
50
0
a
a
a
b
control
F
C60
F+C60

Fig. 5

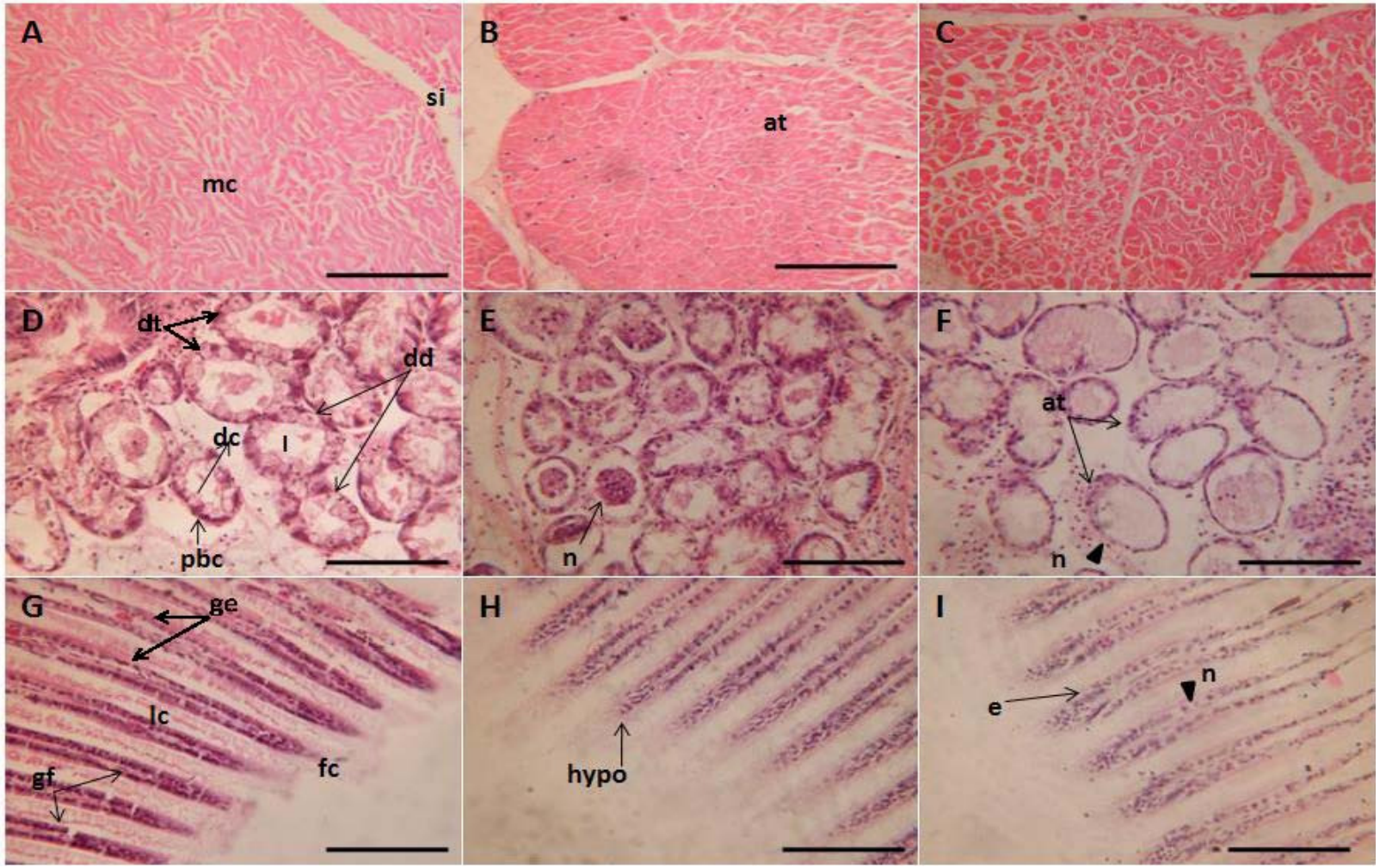

1 Fig. 6

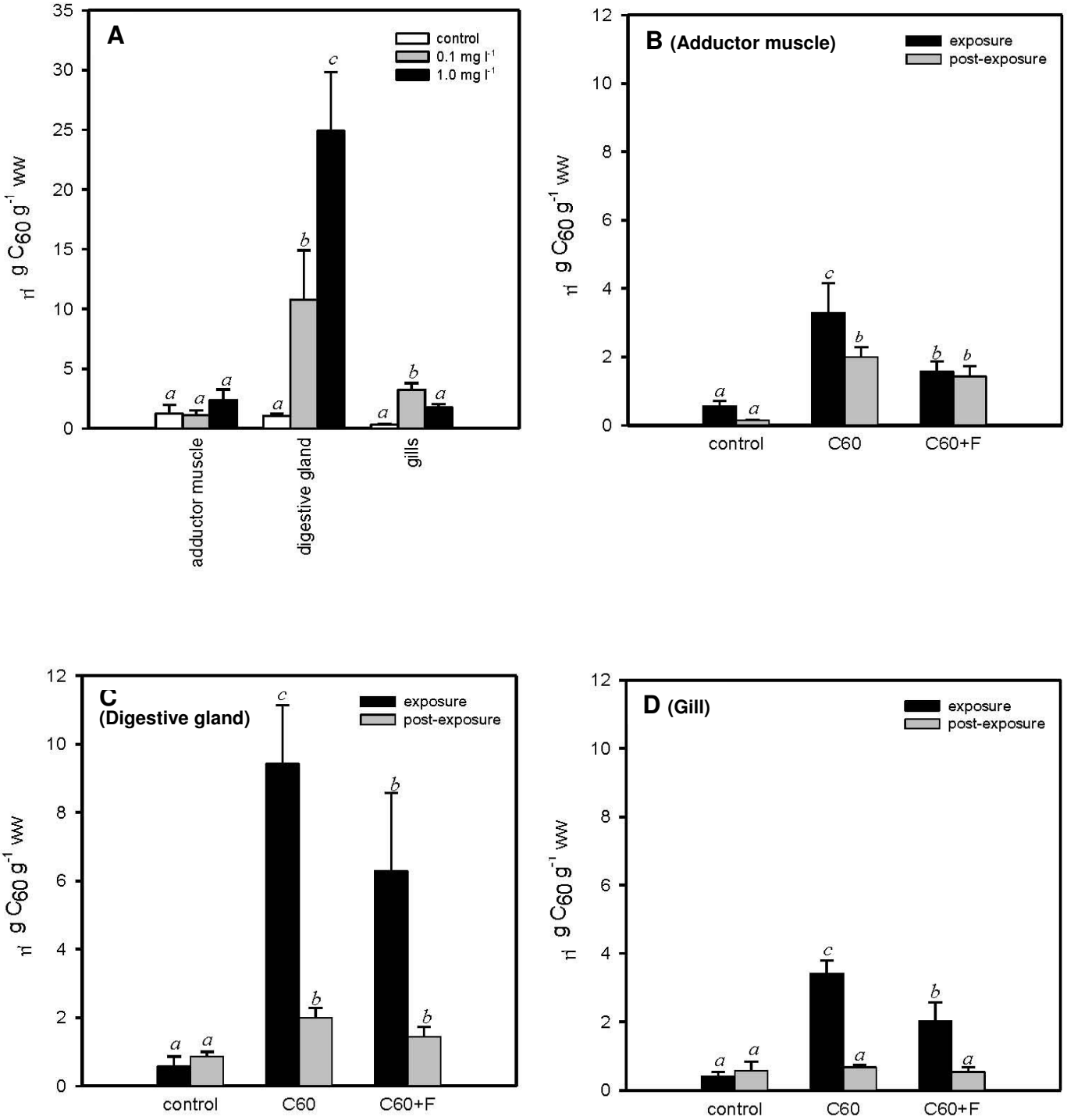
A
control
0.1 mg l-1
1.0 mg l-1
ng g C60 g-1 ww
adductor muscle
digestive gland
gills
B (Adductor muscle)
exposure
post-exposure
control
C60
C60+F
C (Digestive gland)
D (Gill)

2

3

4

5

1 Fig. 7

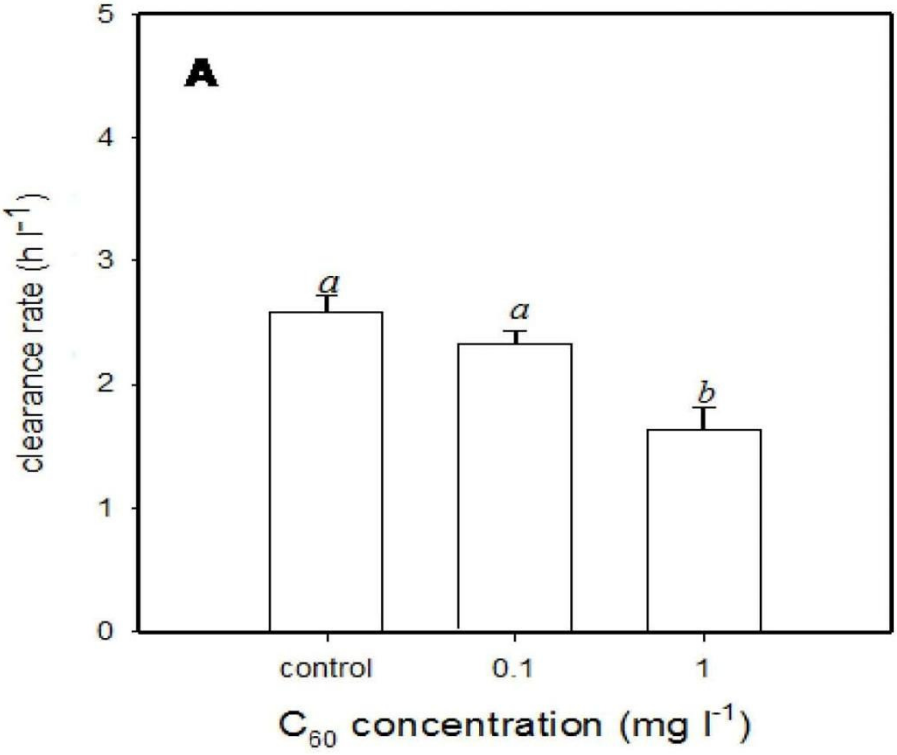
A
clearance rate (h l-1)
5
4
3
2
1
0
a
a
b
control
0.1
1
C60 concentration (mg l-1)

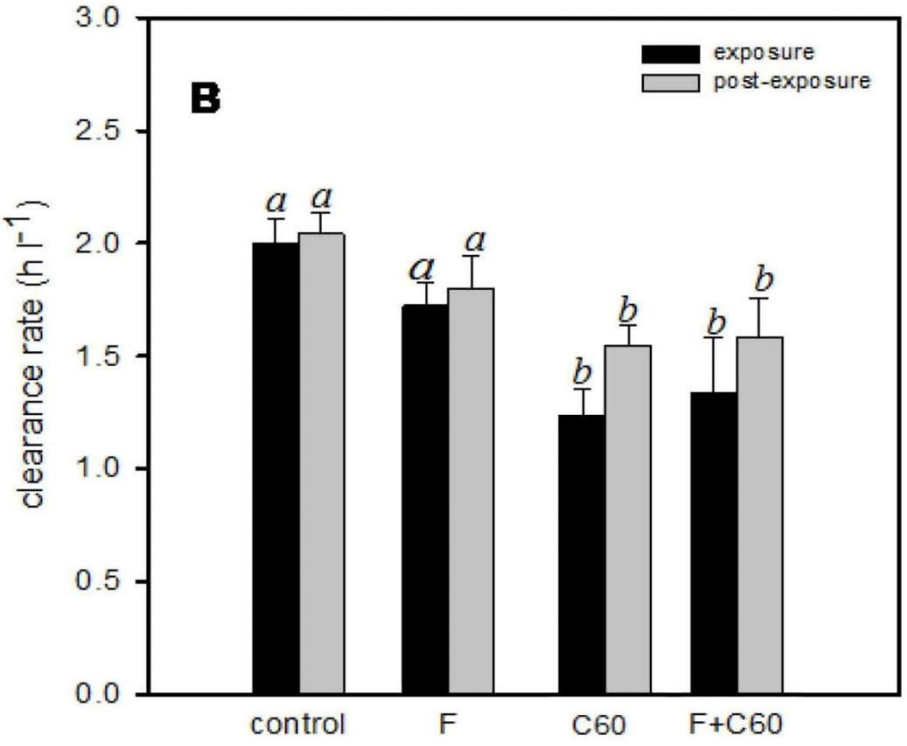
B
exposure
post-exposure
clearance rate (h l-1)
3.0
2.5
2.0
1.5
1.0
0.5
0.0
a a
a a
b b
b b
control
F
C60
F+C60

2